IEEE Access
Multidisciplinary | Rapid Review | Open Access Journal

Received June 14, 2021, accepted June 27, 2021, date of publication June 30, 2021, date of current version July 29, 2021.

Digital Object Identifier 10.1109/ACCESS.2021.3093656

Four-Node Antenna Feeding Network for Interfacing With Differential Front-End Electronics

ILONA PIEKARZ, (Member, IEEE), JAKUB SOROCKI, (Member, IEEE), ROBERT SMOLARZ, SLAWOMIR GRUSZCZYNSKI, (Member, IEEE), AND KRZYSZTOF WINCZA, (Member, IEEE)
Department of Electronics, AGH University of Science and Technology, 30-059 Krakow, Poland

Corresponding author: Ilona Piekarz (ilona.piekarz@agh.edu.pl)

This work was supported by the National Science Center under Contract UMO-2018/31/B/ST7/01718 and Contract UMO-2016/21/B/ST7/02200.

ABSTRACT A novel concept of a differential feeding network for four-node antenna/antenna arrays is proposed. The network is constructed out of a four-strip coupled-line directional coupler operating in a mixed differential-nodal mode enabling direct interfacing of differential front-ends with single-ended antennas. It is shown, that such a configuration provides at the outputs of the proposed feeding network four signals, which are equal in amplitude and with phase progression of 90°. Thus, such a network can be utilized for generating either dual-circular polarization from a 2 × 2 antenna array or can constitute simultaneously two out-of-phase power dividers and a directional coupler resulting in a two-beam antenna array in one cut-plane and two-element array in the other one. The dual-circular excitation is of particular interest for modern-day transceivers as it enables polarization-division-duplex communication. The presented concept is confirmed by measurements of two different antenna arrays operating at 2.5 GHz frequency range featuring dual-circular and dual-beam properties, respectively.

INDEX TERMS Differential coupler, differential feeding network, polarisation-division-duplex, polarization-reconfigurable antenna, multi-beam antennas.

I. INTRODUCTION

Differential components are increasingly being used in analog electronics since they feature superior interference rejection in comparison to their single-ended counterparts. Thus, many examples of differential amplifiers, mixers, filters, and the entire transceiver blocks can be found in the literature [1]–[4]. Following the trend of differential circuits' utilization, also antenna feeding networks connected to modern differential transceivers should operate in a differential mode to avoid balun circuits for balanced-to-unbalanced signal conversion and thus reduce complexity and losses of the network, etc.

The feeding networks in antenna arrays are utilized to integrate different properties such as multiple beams [5] or reconfigurable polarization [6], [7] in a common aperture. Among passive feeding networks, Butler matrices [5], [7]–[9] are very popular. One of the Butler matrix applications is the generation of independent beams featuring a given polarization, either symmetrically located with respect to broadside direction or two symmetrically located together with broadside and end-fire beams [10]–[15]. Another application of such a beamforming network is shown in [16], where four appropriately connected 3-dB/90° directional couplers are utilized for achieving dual-circular polarization from a series-fed antenna lattice. In [17], it is shown that such a beamforming network also allows for achieving dual-beam properties in horizontal and vertical directions. Such a concept has been also applied for the 8 × 8 Butler matrix which allows for achieving 8 beams in two different directions [18]. Nevertheless, the main drawback of this type of beamforming network is its complex construction. For example, N-element antenna array beamforming networks usually require $\frac{N}{2}\left(log_2\left(N\right)\right)$ directional couplers, which means that the beamforming network of a four-element antenna array is composed of four directional couplers [19]. Moreover, in a classical realization,

The associate editor coordinating the review of this manuscript and approving it for publication was Debdeep Sarkar.

the Butler matrix is a single-ended input/output feeding network, which cannot be directly connected to a differential transceiver.

In this paper, we propose for the first time to the best of our knowledge, a novel approach to the design of a beamforming network designated for differential front-end electronics. In the proposed concept, a single element being a four-strip differentially-fed coupled-line directional coupler is used as a feeding network for a four-element antenna array, in which input and isolated ports operate in a differential mode, whereas transmission and coupled ports operate in a decomposed single-ended mode. Such a configuration allows to achieve dual-beam or dual-polarization properties of an antenna array and the dual-circular excitation is of particular interest for modern-day transceivers as it enables polarization-division-duplex communication. The radiating elements are fed with four signals having equal amplitudes among which there are two pairs of out-of-phase signals being simultaneously in quadrature (either 90° or −90° depending on the chosen differential input port) with respect to each other. This is a great advantage in comparison to the classic approaches, in which to obtain dual circular polarization in a four-node antenna four 3-dB quadrature directional couplers are required, whereas to achieve dual-beam properties at least one 3-dB quadrature directional coupler and additionally two power dividers are required. Moreover, the proposed approach decreases the complexity of the feeding network and reduces the occupied area as well as the lengths of signal paths, thus also reduces the insertion losses in circuits, especially when connected with differential RX/TX devices (no additional baluns required). The proposed concept was confirmed by measurements of two antenna arrays operating in the 2.4 GHz frequency range featuring dual-circular polarization and dual-beam properties, respectively.

II. CONCEPT OF FOUR-ELEMENT ANTENNA ARRAYS FED WITH DIFFERENTIAL/NODAL DIRECTIONAL COUPLERS

In modern-day electronics, RF active circuitry such as amplifiers, mixers, or the entire transceiver blocks is designed as differential circuits, as it can be seen in [20]–[24]. Thus to connect them with a single-ended feeding network of an antenna array, even in state-of-the-art realizations such as [25], [26] extra baluns are being used as shown in Fig. 1a. The use of a feeding network featuring a differential interface on the transceiver side as proposed in Fig. 1b addresses the above issue allowing to reduce system complexity, minimize the occupied area, reduce the losses (shorter signal paths, no balun needed), and improve interference immunity. In modern-day telecommunication applications, the above are important concerns.

Following the approach shown in Fig. 1b, a differential interface feeding network for a four-element antenna array is proposed that is realized with a single four-strip coupled-line directional coupler operating in a mixed differential-nodal mode. The base circuit - a differential four-strip coupled-line coupler is shown schematically in Fig. 2a and according

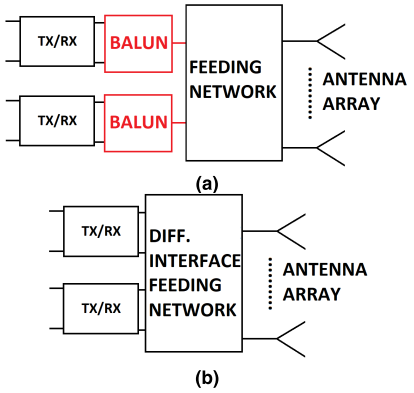

FIGURE 1. (a) Block diagrams presenting the connection of differential transceiver with a single-ended feeding network using baluns and (b) direct connection of differential transceivers with a differential interface feeding network.

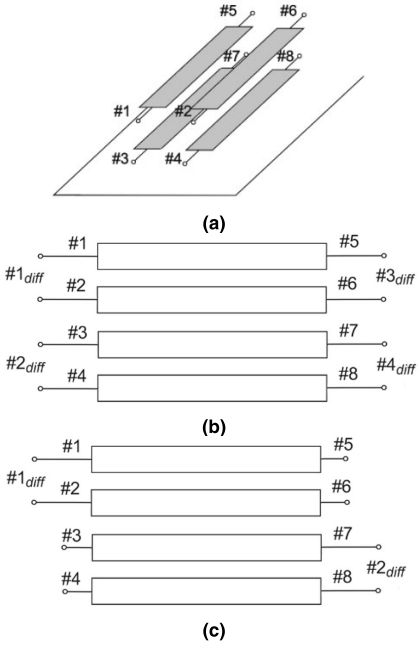

FIGURE 2. (a) Concept of a four-strip coupled-line system constituting a differentially-fed directional coupler, (b) differential excitation of the coupler, and (c) mixed - differential/nodal excitation.

to [27] nodal ports #1, #2 and #5, #6 form the first balanced line, whereas ports #3, #4, and #7, #8 form the second balanced line. The choice of the conductors for each balanced line can be freely selected but the most practical case is when the conductors of each balanced line are on one plane, therefore, nodal ports #1 and #2 form the differential input of the top balanced line, whereas the ports #3 and #4 form the differential port of the lower balanced line. Since the conductors of the lines can be placed one above the other, the directional coupler can easily feature relatively strong coupling. The differential excitation of the coupler is presented in Fig. 2b according to [27], however, for antenna applications interesting is the case of mixed differential/nodal excitation shown in Fig. 2c. In such a configuration the input

ports #1$_{diff}$ (created by nodal ports #1, #2) and #2$_{diff}$ (created by nodal ports #7, #8) are isolated with respect to each other, and the output ports #3, #4, #5, and #6 are the nodal ones, and the signals receiving at these nodal ports can be utilized for excitation of particular radiating elements in an antenna array. It has to be noted, the output ports #3, #4, #5, and #6 are matched to the impedance $Z_{diff}/2$.

The differential coupler presented in Fig. 2 can be described using mixed-mode scattering parameters, which can be converted to the nodal ones S_{nodal}, as presented in Appendix. Applying the differential excitation to one pair of ports, the following response is obtained:

$$\begin{bmatrix} b_1 \\ b_2 \\ b_3 \\ b_4 \\ b_5 \\ b_6 \\ b_7 \\ b_8 \end{bmatrix} = \boldsymbol{S_{nodal}} \frac{1}{\sqrt{2}} \begin{bmatrix} 1 \\ -1 \\ 0 \\ 0 \\ 0 \\ 0 \\ 0 \\ 0 \end{bmatrix} \tag{1}$$

and thus

$$b_1 = b_2 = b_7 = b_8 = 0 \tag{2}$$

$$b_3 = \frac{1}{2\sqrt{2}} \left(C_{diff} + C_{com} + C_{diff} - C_{com}\right) = \frac{1}{\sqrt{2}} C_{diff} \tag{2a}$$

$$b_4 = \frac{1}{2\sqrt{2}} \left(-C_{diff} + C_{com} - C_{diff} - C_{com}\right) = -\frac{1}{\sqrt{2}} C_{diff} \tag{2b}$$

$$b_5 = \frac{1}{2\sqrt{2}} \left(T_{diff} + T_{com} + T_{diff} - T_{com}\right) = \frac{1}{\sqrt{2}} T_{diff} \tag{2c}$$

$$b_6 = \frac{1}{2\sqrt{2}} \left(-T_{diff} + T_{com} - T_{diff} - T_{com}\right) = -\frac{1}{\sqrt{2}} T_{diff} \tag{2d}$$

where b_i is the reflected wave at port # I, while C_{diff} and T_{diff} are differential mode coupling and transmission coefficients. Therefore, for a 3-dB-differential directional coupler in which $C_{diff} = \frac{1}{\sqrt{2}}$, $T_{diff} = \frac{-j}{\sqrt{2}}$, the signals at the four single-ended outputs equal:

$$b_3 = \frac{1}{2}, \quad b_4 = -\frac{1}{2}, \; b_5 = \frac{-j}{2}, \; b_6 = \frac{j}{2} \tag{3}$$

One can notice that the output signals are all equal in amplitude with the phase progression of 90°. Such a feature allows utilization of the differential/nodal directional coupler from Fig. 2c as a differential interface feeding network as shown in Fig. 1b in antenna arrays with dual-beam or dual-polarization properties. Examples of the discussed use-cases where one radiating element is attached to each of the four feeding nodes are provided in Fig. 3. Dual-circular and linear dual-beam arrays are drawn schematically in Fig. 3a and Fig. 3b, respectively.

The first four-element antenna array, presented in Fig. 3a in which dual-circular polarization can be achieved is constructed out of four microstrip patches, which are equally

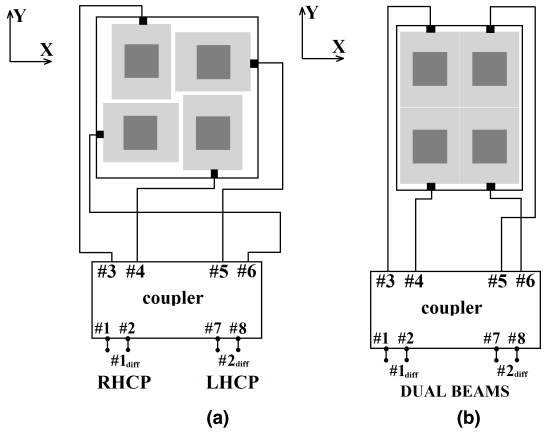

FIGURE 3. Schematic diagram of a four-element antenna fed by the mixed differential/nodal directional coupler (a) featuring dual-circular polarization and (b) dual-beam properties.

spaced by 0.8 λ and sequentially rotated to generate circular polarization. The pairs of nodal outputs that constitute the differential ports (#3 & #4 and #5 & #6) are connected to the patches that have to be fed with out-of-phase signals. Depending on the chosen differential inputs (#1 or #2) there is a ±90° phase shift between these pairs of nodal outputs. Therefore, such an arrangement allows for achieving either RH or LH circular polarization.

The second four-element antenna array presents a concept in which a dual-beam antenna array can be obtained (Fig. 3b). The patches are spaced by 0.5 λ on X-axis and by 0.8 λ on Y-axis. The pairs of nodal outputs that constitute the differential ports (#3 & #4 and #5 & #6) are utilized for feeding two-element columns along Y-axis, whereas ±90° phase shifts between these pairs of nodal outputs are used for achieving dual-beam radiation pattern along X-axis. Therefore, the differential coupler serves in this configuration as a feeding network composed of a classic quadrature directional coupler and two out-of-phase power dividers.

III. DEMONSTRATOR REALIZATION AND EXPERIMENTAL RESULTS

A. DESIGN OF A FEEDING NETWORK COMPOSED OF A DIFFERENTIAL/NODAL DIRECTIONAL COUPLER

To verify the concept presented in Section II, the differential directional coupler was designed following the procedure described in [27]. The cross-sectional view of the proposed feeding network shown schematically in Fig. 2a is shown in Fig. 4. As seen, the circuit is composed of four conductors having width w and spacing s. The dielectric stratification consists of two 60 mils thick top and bottom laminate layers ($h_{1,3}$ = 1.52 mm) and 6 mils thick middle one (h_2 = 0.15 mm), on which the traces of the coupler are etched. All layers have equal dielectric constant $\varepsilon_{r1,2,3} = 3.38$.

Following the design procedure for the differential directional coupler described in [27] iteratively, the coupled-line geometry was optimized to obtain a 3-dB differential directional coupler. The final widths of the conductors and slots

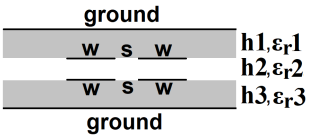

FIGURE 4. Cross-sectional view of the coupled-line geometry utilized for the design of a differential and mixed differential/nodal directional coupler. A three-laminate stripline arrangement was used with full ground planes on both sides. The metal strips feature widths w, whereas the spacing between the strips is equal to s. The layer heights and permittivity are marked as $h_{1,2,3}$ and $\varepsilon_{r1,2,3}$, respectively.

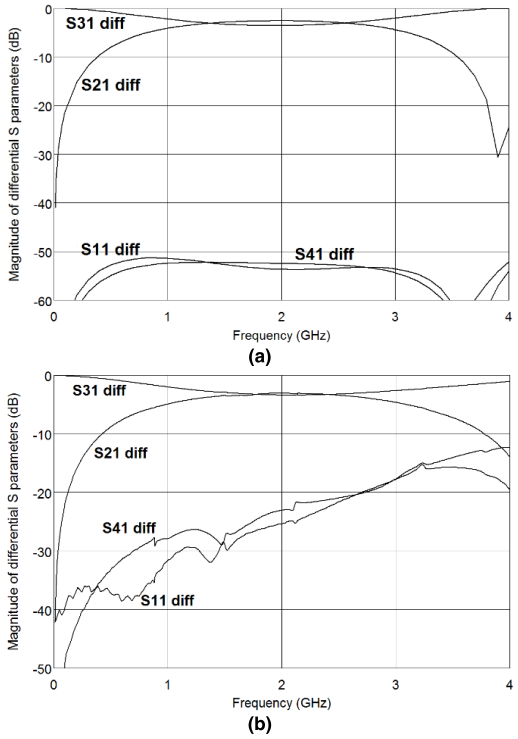

FIGURE 5. (a) Electromagnetically calculated and (b) measured differential scattering parameters of the designed 3-dB differential directional coupler. Port numeration according to Fig. 2b.

between conductors were found for a given stratification to be $w = 0.6$ mm and $s = 1.4$ mm, respectively. The differential scattering parameters of the designed coupled-line geometry (configuration as shown in Fig. 2b) were calculated electromagnetically using *AWR Microwave Office* software and the results are shown in Fig. 5a. The circuit was designed to be matched to $Z_{diff} = 100\ \Omega$.

The coupler features an equal power split in the frequency range of 1.15 GHz - 2.75 GHz with the imbalance between coupling and transmission characteristics not exceeding ± 0.5 dB. The calculated return losses and isolations are as low as -50 dB. The designed directional coupler was manufactured and measured. The measurement results are provided in Fig. 5b. As can be seen from the comparison of calculated and measured results, the coupling and transmission characteristics are in good agreement. The coupling/transmission imbalance decreased from ± 0.5 dB to

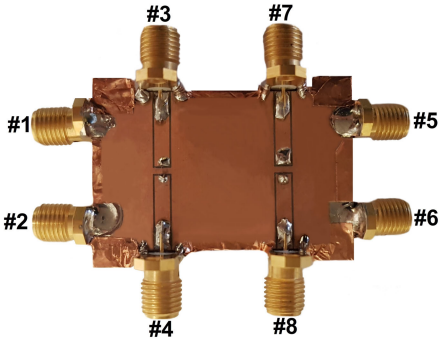

FIGURE 6. Photograph of the manufactured coupler with port numbering as shown in Fig. 2a.

± 0.18 dB. The measured return losses and isolations are better than 25 dB and 22 dB at the center frequency of 2 GHz. A photograph of the manufactured coupler with ports indicated is presented in Fig. 6. Following, the mixed differential/nodal S-parameters of the fabricated coupler were derived to validate its properties in the intended setting as a differential feeding network for a four-node antenna array (see Fig. 2c). The measurement results are shown in Fig. 7. The differential ports $\#1_{diff}$ and $\#2_{diff}$ from Fig. 2c are selected as inputs, whereas the nodal ports #3, #4, #5, and #6 are selected as outputs, for excitation of radiating elements (see Fig. 2c and Fig. 3). In such a mixed excitation the coupler exhibits properties as predicted theoretically in this Section, i.e. the signal is equally split to four output ports. Simultaneously the coupler features good return loss and isolation properties. Moreover, proper phase relations are measured between signals at the output ports, i.e. the phase progression equals 90°, as predicted, what is a necessary feature for application in the antenna arrays described in the proceeding section.

As it was pointed out, the proposed mixed differential/nodal directional coupler is well suited for future telecommunication applications with balanced inputs/outputs of transceivers. However, for concept validation and measurements of the antenna concepts with commonly available Vector Network Analyzer (VNA), extra baluns were added to both differential interfaces ($\#1_{diff}$, $\#2_{diff}$ in Fig. 2c, and Fig. 3) to provide an easy connection between the directional coupler's balanced inputs and the analyzer's nodal inputs. This was due anechoic chamber's hardware setup that incorporates a VNA operating with unbalanced RF signals. The used transmission line baluns operate at the center frequency of 2.5 GHz, however feature narrower bandwidth than the feeding network itself, and therefore the focus was put on the performance at the center frequency of the network. The balun design is outside the scope of this paper.

B. DESIGN OF A SINGLE RADIATION ELEMENT

A single radiating element was designed at first to assembly an antenna array and verify experimentally the concept presented in Section II. A well-known aperture coupled microstrip patch antenna shown in Fig. 8 was designed to minimize the number of factors that can affect the

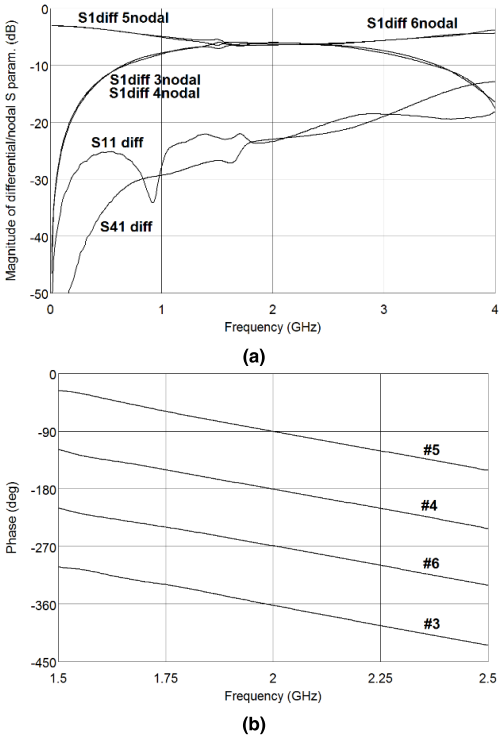

FIGURE 7. Measured mixed scattering parameters of the fabricated directional coupler. The measurement has been made with differentially excited input ports and the output signals have been measured with respect to the common ground (nodal excitation). (a) Amplitude characteristics and (b) phase characteristics. Port numeration as indicated in Fig. 2c.

performance of the constructed 2 × 2 antenna array. The dielectric stratification (Fig. 8b) consists of two 30 mils thick laminate layers having dielectric constant $\varepsilon_{r1,3} = 2.5$ and a 393.7 mil thick air layer. The feeding line was etched on the metal layer m3, while the patch on the metal layer m1. The size of the patch equals 42.68 × 42. 68 mm, whereas the slot in the ground plane is 30.3-mm long and 7.07-mm wide. The width of the 50-Ω feeding line is equal to 2.16 mm and it excites the center of the slot with an 8 mm stub to achieve a good reflection coefficient. The designed radiating element was manufactured and measured with the results shown in Fig. 9, i.e. measured impedance match, radiation pattern @ 2.5 GHz, and gain of the model. A seen, the radiating patch operates at the center frequency of 2.5 GHz and features a bandwidth of about 400 MHz due to suspending the patch over a thick air layer, while it is still within and almost 4 times lower of that for the feeding network. Four of such radiation elements were used for the realization of 2 × 2 antenna arrays.

C. EXPERIMENTAL VERIFICATION OF 2 × 2 ANTENNA ARRAY FEATURING DUAL-CIRCULAR POLARIZATION OR DUAL-BEAM RADIATION PATTERN

To validate the polarization reconfigurability feeding scheme, the developed feeding network was connected with a 2 × 2 antenna array in a way shown schematically in Fig. 3a.

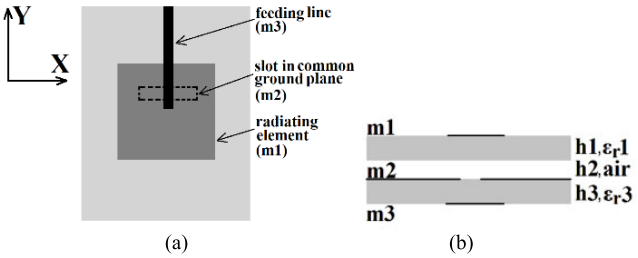

FIGURE 8. (a) Layout and (b) dielectric stack-up of an aperture coupled microstrip patch utilized to construct and experimentally verify a four-element antenna array and feeding network beamforming properties.

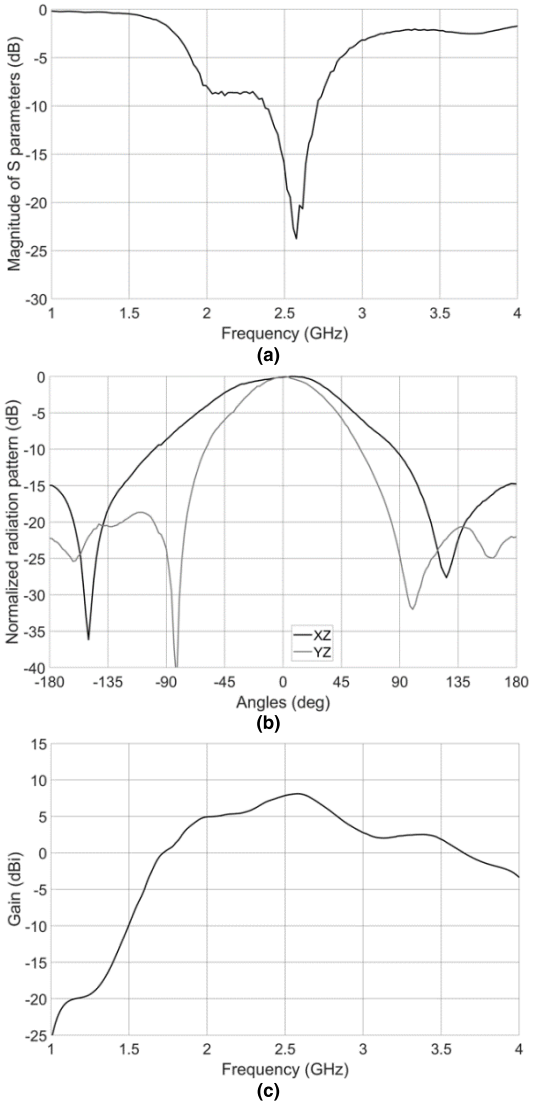

FIGURE 9. (a) Measured impedance match, (b) radiation pattern @ 2.5 GHz (b), and (c) maximum gain of an exemplary fabricated single radiating element used in the experiment.

The array was verified by EM simulations using *Ansys HFSS* software as well as by measurements of the assembled model. The comparison of the radiation patterns at 2.5 GHz obtained with EM simulations and by measurements

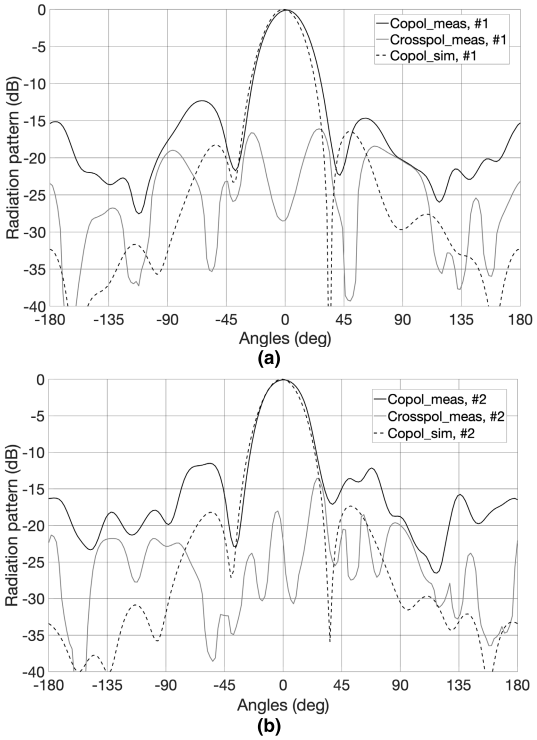

FIGURE 10. Radiation pattern @ 2.5 GHz of the developed four-element antenna array featuring dual-circular polarization obtained when (a) the signal is provided to port #1 (RHCP) and (b) to port #2 (LHCP). Measurement results – solid lines, simulation results – dashed lines.

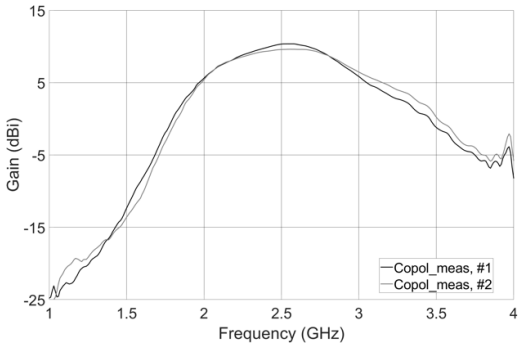

FIGURE 11. Measured gain of the developed four-element antenna array featuring dual-circular polarization and realized with the use of a mixed differential/nodal directional coupler-based feeding network when either port #1_{diff} or #2_{diff} is excited. Note that from a broadband operation perspective, the gain is affected by the use of baluns.

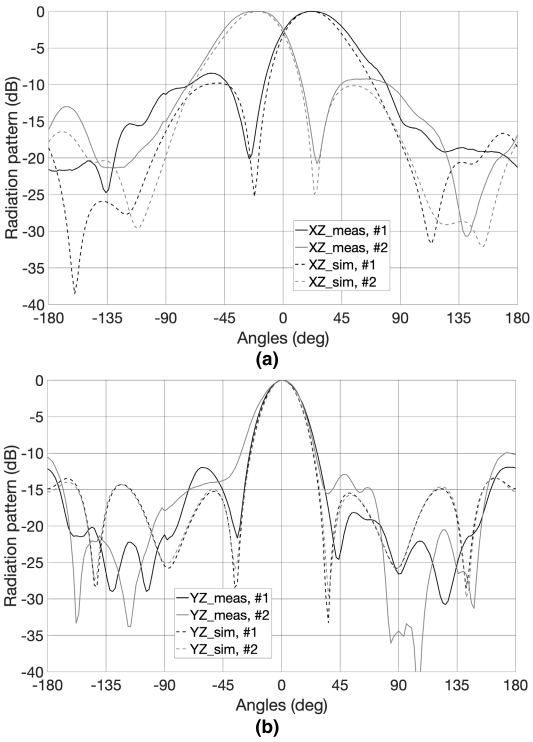

FIGURE 12. The radiation pattern of the developed four-element antenna array @ 2.5 GHz featuring dual-beam properties and realized with the use of a mixed differential/nodal directional coupler obtained in (a) XZ cut-plane and (b) YZ cut-plane. Measurement results – solid lines, simulation results – dashed lines.

are shown in Fig. 10, where normalized radiation patterns for RH and LH circular polarization are provided. Figure 11 shows the measured maximum gain vs. frequency for both input ports. As seen from the measurement results, identical beamwidth was achieved for both the RHCP and the LHCP polarization. The measurement results are in good agreement with the simulated ones.

Beam widths of the measured radiation patterns are equal to 32 deg and are 4 deg wider in comparison to the beam widths of the EM simulated patterns. Moreover, the measured sidelobe level does not exceed 12 dB. The maximum gain of the realized antenna array exceeds 10.4 dBi at the center frequency (7.8 dBi measured for a single element with linear polarization).

Following, to validate the multibeam feeding scheme, the developed feeding network was connected with a 2 $\times$ 2 antenna array in a way shown schematically in Fig. 3b. Again, the array was verified by EM simulations using *Ansys HFSS* software as well as by measurements of the assembled model. The comparison of the radiation patterns at 2.5 GHz obtained with EM simulations and by measurements are shown in Fig. 12, where normalized radiation patterns in two principal cut-planes are presented. Figure 13 shows the measured maximum gain vs. frequency for both input ports.

As seen, the developed antenna array features dual-beam properties in the XZ cut-plane and the measurement results are in good agreement with the simulated ones. The beam can be directed at either $+20$ deg or -20 deg and the measured data matches the simulated one. The sidelobe level is better than 9.8 dB for the EM simulated antenna array which is lower than the theoretical value of 12 dB due to the array elements' sub-optimal spacing. The measured sidelobe level is better than 8 dB, which can be attributed to a slight difference in phase progressions in the manufactured feeding network due to finite fabrication and assembly tolerances. Beam widths of the measured radiation patterns in the XZ cut-plane are equal to 50 deg and are 6 deg wider in comparison

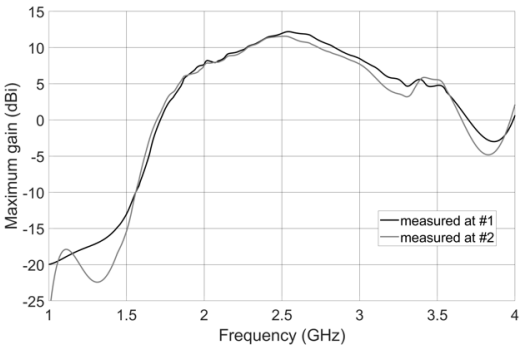

FIGURE 13. The measured maximum gain of the developed four-element antenna array @ 2.5 GHz featuring dual-beam properties and realized with the use of a mixed differential/nodal directional coupler-based feeding network when either port #1$_{diff}$ or #2$_{diff}$ is excited. Note that from a broadband operation perspective, the gain is affected by the use of baluns.

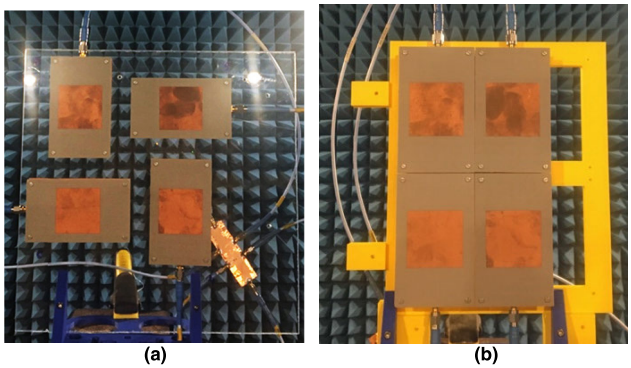

FIGURE 14. Photographs of the assembled experimental antenna arrays mounted in the anechoic chamber: the one featuring (a) Dual-Circular Polarization (a) and the one featuring (b) Dual-Beam Radiation.

to the beam widths of the EM simulated radiation patterns. The measured gain exceeds 12.3 dBi. Photographs of the two realizations of a 2 × 2 antenna array with different radiation features are shown in Fig. 14.

IV. DISCUSSION

The proposed feeding network features a differential interface between TX/RX devices and a four-node antenna array. In the presented approach a single differential coupler is utilized to deliver signals that excite dual circular polarization or dual-beam properties in a four-node antenna array when the coupler is used in the mixed differential-nodal configuration. To present the advantages of the proposed feeding network, two application cases should be considered:

1) RX/TX circuits are single-ended interface devices,
2) RX/TX circuits are differential interface devices.

In the first case in classic approaches, to obtain dual circular polarization in a four-node antenna array arranged in a 2 × 2 array, four 3-dB quadrature directional couplers are required, as was shown in [28]. Similarly, to achieve dual-beam properties in a four-node antenna array at least one 3-dB quadrature directional coupler and additionally, two power dividers are required. In opposite to the solutions described in the literature, the proposed network is constructed out of a single differential coupler which requires two additional balun circuits to be added to connect single-ended RX/TX devices. Thus, the resulting feeding network features less (dual-polarization properties) or the same number (dual-beam properties) of building elements, than in classic approaches. Moreover, the proposed approach decreases the complexity of the feeding network and reduces the occupied area as well as the lengths of signal paths, thus also reduces the insertion losses in circuits.

For the latter case which is the most often used configuration in modern-day telecommunication applications the advantage of the proposed differential coupler feeding network is even greater. In such a case no additional baluns are required to be added to connect RX/TX devices and dual circular polarization or dual-beam properties are realized using a single differential coupler. Such an approach can significantly reduce the system complexity and total power losses. Therefore, it can be stated that the proposed network features significant advantages comparing to the known solutions, and is especially desirable in modern-day wireless systems with differential TX/RX interface.

V. CONCLUSION

A novel concept of a four-node antenna feeding network for interfacing with differential front-end electronics based on a single, mixed differential/nodal directional coupler was introduced. It was shown that such a single directional coupler can be efficiently utilized as a feeding network of a four-element antenna array that features either dual-beam or dual-circular polarization properties. The proposed concept has been verified by measurements of two antenna arrays operating at the center frequency of 2.5 GHz and the obtained measurement results fully confirm the presented approach. It has to be underlined, the presented concept has additional advantages in modern millimeter-wave wireless systems where reduction of system complexity due to uniform differential-mode operation contributes strongly to the reduction of physical size and total power losses with improvement in system interference immunity, which are of concern.

APPENDIX

The considered differentially excited directional coupler, shown in Fig. 2, can be described with the following mixed-mode scattering matrix:

$$\boldsymbol{S}_{mixed\ mode} = \begin{bmatrix} \boldsymbol{S}_{diff} & 0 \\ 0 & \boldsymbol{S}_{com} \end{bmatrix} \tag{4}$$

where $\boldsymbol{S}_{diff}$ and $\boldsymbol{S}_{com}$ are the 4 × 4 submatrices describing differential- and common-mode scattering parameters, respectively. The submatrices for an ideal directional coupler, having ideal return losses and ideal isolations are expressed as:

$$S_{diff} = \begin{bmatrix} 0 & C_{diff} & T_{diff} & 0 \\ C_{diff} & 0 & 0 & T_{diff} \\ T_{diff} & 0 & 0 & C_{diff} \\ 0 & T_{diff} & C_{diff} & 0 \end{bmatrix} \tag{4a}$$

$$S_{nodal} = \frac{1}{2}\begin{bmatrix} 0 & 0 & C_{diff}+C_{com} & -C_{diff}+C_{com} & T_{diff}+T_{com} & -T_{diff}+T_{com} & 0 & 0 \\ 0 & 0 & -C_{diff}+C_{com} & C_{diff}+C_{com} & -T_{diff}+T_{com} & T_{diff}+T_{com} & 0 & 0 \\ C_{diff}+C_{com} & -C_{diff}+C_{com} & 0 & 0 & 0 & 0 & T_{diff}+T_{com} & -T_{diff}+T_{com} \\ -C_{diff}+C_{com} & C_{diff}+C_{com} & 0 & 0 & 0 & 0 & -T_{diff}+T_{com} & T_{diff}+T_{com} \\ T_{diff}+T_{com} & -T_{diff}+T_{com} & 0 & 0 & 0 & 0 & C_{diff}+C_{com} & -C_{diff}+C_{com} \\ -T_{diff}+T_{com} & T_{diff}+T_{com} & 0 & 0 & 0 & 0 & -C_{diff}+C_{com} & C_{diff}+C_{com} \\ 0 & 0 & T_{diff}+T_{com} & -T_{diff}+T_{com} & C_{diff}+C_{com} & -C_{diff}+C_{com} & 0 & 0 \\ 0 & 0 & -T_{diff}+T_{com} & T_{diff}+T_{com} & -C_{diff}+C_{com} & C_{diff}+C_{com} & 0 & 0 \end{bmatrix} \tag{7}$$

$$S_{com} = \begin{bmatrix} 0 & C_{com} & T_{com} & 0 \\ C_{com} & 0 & 0 & T_{com} \\ T_{com} & 0 & 0 & C_{com} \\ 0 & T_{com} & C_{com} & 0 \end{bmatrix} \tag{4b}$$

where T_x and C_x are transmissions and couplings of the coupler for the respective mode.

Having found the mixed-mode scattering matrix one can easily convert it to a nodal scattering matrix [27]:

$$\boldsymbol{S}_{nodal} = \boldsymbol{M}^{-1}\boldsymbol{S}_{mixed\ mode}\boldsymbol{M} \tag{5}$$

where:

$$\boldsymbol{M} = \frac{1}{\sqrt{2}}\begin{bmatrix} 1 & -1 & 0 & 0 & 0 & 0 & 0 & 0 \\ 0 & 0 & 1 & -1 & 0 & 0 & 0 & 0 \\ 0 & 0 & 0 & 0 & 1 & -1 & 0 & 0 \\ 0 & 0 & 0 & 0 & 0 & 0 & 1 & -1 \\ 1 & 1 & 0 & 0 & 0 & 0 & 0 & 0 \\ 0 & 0 & 1 & 1 & 0 & 0 & 0 & 0 \\ 0 & 0 & 0 & 0 & 1 & 1 & 0 & 0 \\ 0 & 0 & 0 & 0 & 0 & 0 & 1 & 1 \end{bmatrix} \tag{6}$$

The resulting nodal matrix is shown in (7) at the top of the page.

REFERENCES

[1] B. Sewiolo, G. Fischer, and R. Weigel, "A 30 GHz variable gain amplifier with high output voltage swing for ultra-wideband radar," *IEEE Microw. Wireless Compon. Lett.*, vol. 19, no. 9, pp. 590–592, Sep. 2009.

[2] E. Laskin, M. Khanpour, S. T. Nicolson, A. Tomkins, P. Garcia, A. Cathelin, D. Belot, and S. P. Voinigescu, "Nanoscale CMOS transceiver design in the 90–170-GHz range," *IEEE Trans. Microw. Theory Techn.*, vol. 57, no. 12, pp. 3477–3490, Dec. 2009.

[3] X. Gao, W. Feng, and W. Che, "High-selectivity wideband balanced filters using coupled lines with open/shorted stubs," *IEEE Microw. Wireless Compon. Lett.*, vol. 27, no. 3, pp. 260–262, Mar. 2017.

[4] W. Zhang, Y. Wu, Y. Liu, C. Yu, A. Hasan, and F. M. Ghannouchi, "Planar wideband differential-mode bandpass filter with common-mode noise absorption," *IEEE Microw. Wireless Compon. Lett.*, vol. 27, no. 5, pp. 458–460, May 2017.

[5] J. Butler and R. Lowe, "Beam-forming matrix simplifies design of electronically scanned antennas," *Electron. Des.*, vol. 9, pp. 170–173, Apr. 1961.

[6] S.-H. Hsu, Y.-J. Ren, and K. Chang, "A dual-polarized planar-array antenna for S-band and X-band airborne applications," *IEEE Antennas Propag. Mag.*, vol. 51, no. 4, pp. 70–78, Aug. 2009.

[7] I. Slomian, K. Wincza, and S. Gruszczynski, "Series-fed microstrip antenna lattice with switched polarization utilizing Butler matrix," *IEEE Trans. Antennas Propag.*, vol. 62, no. 1, pp. 145–152, Jan. 2014.

[8] C. Dall'Omo, T. Monediere, B. Jecko, F. Lamour, I. Wolk, and M. Elkael, "Design and realization of a 4×4 microstrip Butler matrix without any crossing in millimeter waves," *Microw. Opt. Technol. Lett.*, vol. 38, no. 6, pp. 462–465, Sep. 2003.

[9] S. Gruszczynski, K. Wincza, and K. Sachse, "Reduced sidelobe four-beam N-element antenna arrays fed by 4×N Butler matrices," *IEEE Antennas Wireless Propag. Lett.*, vol. 5, no. 1, pp. 430–434, Dec. 2006.

[10] B. Cetinoneri, Y. A. Atesal, and G. M. Rebeiz, "An 8×8 Butler matrix in 0.13-μm CMOS for 5–6-GHz multibeam applications," *IEEE Trans. Microw. Theory Tech.*, vol. 59, no. 2, pp. 295–301, Feb. 2011.

[11] T.-Y. Chin, J.-C. Wu, S.-F. Chang, and C.-C. Chang, "A V-band 8×8 CMOS Butler matrix MMIC," *IEEE Trans. Microw. Theory Tech.*, vol. 58, no. 12, pp. 3538–3546, Dec. 2010.

[12] K. Wincza, S. Gruszczynski, and K. Sachse, "Broadband planar fully integrated 8×8 Butler matrix using coupled-line directional couplers," *IEEE Trans. Microw. Theory Tech.*, vol. 59, no. 10, pp. 2441–2446, Oct. 2011.

[13] M. Koubeissi, C. Decroze, T. Monediere, and B. Jecko, "Switched-beam antenna based on novel design of Butler matrices with broadside beam," *Electron. Lett.*, vol. 41, no. 20, pp. 1097–1098, Sep. 2005.

[14] P. Kaminski, K. Wincza, and S. Gruszczynski, "Switched-beam antenna array with broadside beam fed by modified Butler matrix for radar receiver application," *Microw. Opt. Technol. Lett.*, vol. 56, no. 3, pp. 732–735, Mar. 2014.

[15] S. Gruszczynski, K. Wincza, and K. Sachse, "Broadband 4×4 Butler matrix utilizing tapered-line directional couplers," in *Proc. Microw., Radar Remote Sens. Symp. (MRRS)*, 2011, pp. 77–81.

[16] I. Slomian, K. Wincza, and S. Gruszczynski, "Polarization purity improvement method for linear series-fed antenna arrays," in *Proc. 10th Eur. Conf. Antennas Propag. (EuCAP)*, Apr. 2016, pp. 1–4.

[17] I. Slomian, K. Wincza, and S. Gruszczynski, "Single-layer four-beam microstrip antenna array," in *Proc. IEEE Radio Wireless Symp. (RWS)*, Jan. 2017, pp. 29–31.

[18] I. Slomian, K. Wincza, K. Staszek, and S. Gruszczynski, "Folded single-layer 8×8 Butler matrix," *J. Electromagn. Waves Appl.*, vol. 31, no. 14, pp. 1386–1398, Jul. 2017.

[19] T. M. Macnamara, "Positions and magnitudes of fixed phase shifters in Butler matrices incorporating 90 degrees hybrids," *IEE Proc. H, Microw., Antennas Propag.*, vol. 135, no. 5, pp. 359–360, Oct. 1988.

[20] J. Y.-C. Liu, J.-S. Chen, C. Hsia, P.-Y. Yin, and C.-W. Lu, "A wideband inductorless single-to-differential LNA in 0.18 μm CMOS technology for digital TV receivers," *IEEE Microw. Wireless Compon. Lett.*, vol. 24, no. 7, pp. 472–474, Jul. 2014.

[21] S. Chen and Q. Xue, "Compact triple-transistor Doherty amplifier designs: Differential/power combining," *IEEE Trans. Microw. Theory Techn.*, vol. 61, no. 5, pp. 1957–1963, May 2013.

[22] F. Gatta, E. Sacchi, F. Svelto, P. Vilmercati, and R. Castello, "A 2-dB noise figure 900-MHz differential CMOS LNA," *IEEE J. Solid-State Circuits*, vol. 36, no. 10, pp. 1444–1452, Oct. 2001.

[23] K. Schmalz, J. Borngraber, Y. Mao, H. Rucker, and R. Weber, "A 245 GHz LNA in SiGe technology," *IEEE Microw. Wireless Compon. Lett.*, vol. 22, no. 10, pp. 533–535, Oct. 2012.

[24] A. Bevilacqua, C. Sandner, A. Gerosa, and A. Neviani, "A fully integrated differential CMOS LNA for 3-5-GHz ultrawideband wireless receivers," *IEEE Microw. Wireless Compon. Lett.*, vol. 16, no. 3, pp. 134–136, Mar. 2006.

[25] A. H. Naqvi and S. Lim, "Review of recent phased arrays for millimeter-wave wireless communication," *Sensors*, vol. 18, no. 10, p. 3194, Sep. 2018.
[26] J. Pang, R. Wu, Y. Wang, M. Dome, H. Kato, H. Huang, A. T. Narayanan, H. Liu, B. Liu, T. Nakamura, and T. Fujimura, "A 28-GHz CMOS phased-array transceiver based on LO phase-shifting architecture with gain invariant phase tuning for 5G new radio," *IEEE J. Solid-State Circuits*, vol. 54, no. 5, pp. 1228–1242, May 2019.
[27] K. Staszek, K. Wincza, and S. Gruszczynski, "Rigorous approach for design of differential coupled-line directional couplers applicable in integrated circuits and substrate-embedded networks," *Sci. Rep.*, vol. 6, no. 1, pp. 1–12, Apr. 2016.
[28] I. Slomian, K. Wincza, and S. Gruszczynski, "Compact integrated feeding network for excitation of dual-circular polarization in series-fed antenna lattice," *IEEE Trans. Antennas Propag.*, vol. 62, no. 11, pp. 5876–5879, Nov. 2014.

ILONA PIEKARZ (Member, IEEE) received the M.Sc. and Ph.D. degrees in electrical engineering from the AGH University of Science and Technology, Krakow, Poland, in 2013 and 2018, respectively.

Since 2011, she has been cooperating with the Microwave Research Group, Department of Electronics, AGH UST, where she has been an Assistant Professor, since 2020. She was a Visiting Student with the Ilmenau University of Technology, Ilmenau, Germany, in 2012. She was a Visiting Researcher with Michigan State University, East Lansing, MI, USA, in 2017. She was employed as a Systems Engineer for ADAS mm-wave radars in the automotive industry, in 2019. She was a Postdoctoral Researcher with the AGH UST, in 2020. From 2020 to 2021, she was a Visiting Postdoctoral Researcher with the University of Pavia, Pavia, Italy. She has coauthored over 60 publications in peer-reviewed journals and conferences. Her research interests include development of sensors and measurement systems in strip transmission line technique for industrial and biomedical applications that take advantage of both subtractive and additive fabrication techniques.

Dr. Piekarz is a member of the IEEE MTTS and EuMA. She also serves as a reviewer for a number of IEEE Transactions and letters.

JAKUB SOROCKI (Member, IEEE) received the M.Sc. and Ph.D. degrees in electrical engineering from the AGH University of Science and Technology (AGH UST), Krakow, Poland, in 2013 and 2018, respectively.

Since 2012, he has been cooperating with the Microwave Research Group, Department of Electronics, AGH UST, where he has been an Assistant Professor, since 2020. He was a Visiting Student with the Ilmenau University of Technology, Ilmenau, Germany, in 2012. He was a Visiting Researcher with Michigan State University, East Lansing, MI, USA, in 2017. He was employed as a Systems Engineer for ADAS mm-wave radars in the automotive industry, in 2019. He was a Postdoctoral Researcher with the AGH UST, in 2020. From 2020 to 2021, he was a Visiting Postdoctoral Researcher with the University of Pavia, Pavia, Italy. He has coauthored over 60 publications in peer-reviewed journals and conferences. His research interests include development of low-loss and high-performance microwave circuits in strip transmission line techniques employing subtractive and additive technologies.

Dr. Sorocki is a member of the IEEE MTTS and EuMA. He also serves as a reviewer for a number of IEEE Transactions and letters.

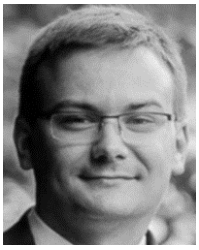

ROBERT SMOLARZ received the M.Sc. degree in electronics and telecommunications with specialization in RF electronics from the Silesian University of Technology, Gliwice, Poland, in 2014. He is currently pursuing the Ph.D. degree with the AGH University of Science and Technology (AGH UST), Krakow, Poland. Since 2015, he has been associated with AGH UST. He is a member of the Microwave Research Group, Department of Electronics, AGH UST. He has three years of industrial experience in cellular networks development. He has coauthored several journal articles and conference papers. His current research interests include development of high-performance microwave passive components utilized in power division circuits, and monolithic microwave integrated circuits (MMIC) design.

SLAWOMIR GRUSZCZYNSKI (Member, IEEE) received the M.Sc. and Ph.D. degrees in electronics and electrical engineering from the Wroclaw University of Technology, Wroclaw, Poland, in 2001 and 2006, respectively. From 2001 to 2006, he was with the Telecommunications Research Institute, Wroclaw. From 2005 to 2009, he was with the Institute of Telecommunications, Teleinformatics, and Acoustics, Wroclaw University of Technology. He joined the Faculty of Informatics, Electronics, and Telecommunications, AGH University of Science and Technology, Krakow, Poland, in 2009, where he has been the Head of the Department of Electronics, since 2012. He has coauthored over 40 journal articles and 50 conference scientific papers. He is also a member of the Committee of Electronics and Telecommunications, Polish Academy of Sciences (PAN).

KRZYSZTOF WINCZA (Member, IEEE) received the M.Sc. and Ph.D. degrees in electronics and electrical engineering from the Wroclaw University of Technology, Poland, in 2003 and 2007, respectively, and the D.Sc. degree (habilitation) from the Department of Electronics, AGH University of Science and Technology, Krakow, Poland, in 2012.

He joined the Institute of Telecommunications, Teleinformatics and Acoustics, Wroclaw University of Technology, in 2007. Since 2009, he has been an Assistant Professor with the Department of Electronics, AGH University of Science and Technology. He attended the Training Program with Stanford University, USA, in 2012. He has coauthored over 40 journal articles and over 50 scientific conference papers. His current research interests include analysis and development of microwave passive devices, such as ultra-broadband directional couplers, microstrip antenna arrays and composite right-left handed artificial transmission lines, as well as multiport reflectometers. From 2014 to 2019, he was a member of the Editorial Boards of the IEEE Microwave and Wireless Components Letters and the Technical Program Committee of the International Conference on Microwaves, Radar, and Wireless Communications (MIKON). He was a recipient of The Youth Award presented at the 10th National Symposium of Radio Sciences (URSI), in 2001, and the Young Scientist Grant awarded by the Foundation for Polish Science, in 2008. He served as an Expert of the European Union COST 284 Project, from 2003 to 2006, and the Polish National Science Center, from 2012 to 2014.